Journal of Non-Crystalline Solids 447 (2016) 9–15

Contents lists available at ScienceDirect

Journal of Non-Crystalline Solids

journal homepage: www.elsevier.com/locate/jnoncrysol

Structural evolution of nickel oxide silica sol-gel for the preparation of interlayer-free membranes

Adi Darmawan [a,*], Linda Karlina [a], Yayuk Astuti [a], Sriatun [a], Julius Motuzas [b], David K. Wang [b], João C. Diniz da Costa [b]

[a] Diponegoro University, Department of Chemistry, Semarang 50275, Indonesia
[b] The University of Queensland, FIM²Lab-Functional Interfacial Materials and Membranes Laboratory, School of Chemical Engineering, Brisbane, Qld 4072, Australia

ARTICLE INFO

Article history:
Received 26 January 2016
Received in revised form 11 May 2016
Accepted 14 May 2016
Available online 20 May 2016

Keywords:
Sol-gel
Nickel oxide
Silica
Membranes
Desalination

ABSTRACT

This work investigates a modified sol-gel method for the preparation of interlayer-free nickel oxide silica membranes for desalination applications. The sol–gels were synthesized using TEOS, nickel nitrate hexahydrate, ethanol as solvent and water with and without peroxide (H_2O_2). The effect of the nickel embedded in the silica matrix as Ni/Si molar ratio was varied from 5 to 50 mol% and systematically studied. The sols prepared with H_2O_2 resulted in microporous structures and lower pore volume, contrary to the mesoporous structures derived from sols without H_2O_2. The modified sol-gel method proved to be robust enough for coating directly on α-alumina substrates, as opposed to conventional methods which required substrates with interlayers. All interlayer-free nickel oxide silica membranes delivered high salt rejection ranging from 91.5 to 99.9%, and reaching water flux as high as 7.3 kg m^{-2} h^{-1}. The membranes prepared using sols with H_2O_2 gave lower water flux and slightly higher salt rejection, attributed to lower pore volume and smaller pore size, respectively. The membranes prepared with Ni/Si molar ratio of 25% achieved the highest water flux, though salt rejection slightly decreased with the increase of feed salt concentration from brackish (NaCl 0.3 wt%) to sea water (NaCl 3.5 wt%).

© 2016 Elsevier B.V. All rights reserved.

1. Introduction

The world is facing a global water crisis due to population growth and climate change [1]. As fresh water resources become scarce and global population is on the increase, the use of seawater desalination technology presents a viable choice in the provision of clean and fresh water [2]. In terms of commercial applications, reverse osmosis (RO) polymeric membranes are still dominating the market [3] despite fouling and cleaning chemical stability limitations [4,5]. To address these limitations, novel inorganic membranes have been considered for desalination applications, including zeolite and silica membranes. The potential use of these membranes is dependent upon their performance in terms of water fluxes and salt rejection. Zeolite membranes generally have low water fluxes around 1 kg m^{-2} h^{-1} [6,7] whilst recent works showed that the membrane instability and loss of salt rejection was attributed to ion exchange with the zeolite cage [8,9].

The potential for silica membranes for liquid processing in pervaporation was envisaged as early as 1990s [10], though research into silica membranes for desalination has been gathering pace in the last decade. Duke and co-workers [11] tested silica membranes prepared by an acid-catalysed sol-gel method in a pervaporation set up which delivered high salt rejection 98% though water fluxes were low at 1.8 kg m^{-2} h^{-1}. The major advantage of silica membranes is pore size control at molecular sieve dimensions. Hence, the smaller pore sizes generally exclude the permeation of the larger hydrated salt ions (hydrated Cl^- 6.64 Å and Na^+ 7.16 Å) [12,13], whilst allowing the preferential permeation of the smaller water molecule ($d_k = 2.6$ Å). However, silica materials contain silanol groups (Si—OH) which are hydrophilic and easily hydrolysed by water [14,15]. As a result, the silica membranes become unstable when exposed to water, rendering the membranes ineffective for desalination applications as demonstrated by Elma et al. [16]. To address this problem, hybrid silica membranes were prepared with carbon templates such as surfactants [17,18] and triblock co-polymers [19], where the organic template was carbonised into carbon moieties inside the silica matrix, or using organo-silica precursors [20,21] to introduce non-hydrophilic C—C bridges between silicon atoms in order to reduce propensity of water hydrolysis.

Further developments on silica derived membranes for desalination were based on doping silica with metal oxides. Lin et al. [22] reported for the first time that cobalt oxide silica membranes were able to desalt water up to NaCl 15 wt%. Recently Elma et al. [23] prepared for the first time interlayer-free cobalt oxide silica membranes where hydro-stability increase with the content of cobalt. Tsuru's group [24] showed that cobalt oxide silica materials were more hydro-stable due to the reduction of thermal vibration by cobalt oxides embedded in the silica matrix.

* Corresponding author.
E-mail address: adi_darmawan@undip.ac.id (A. Darmawan).

http://dx.doi.org/10.1016/j.jnoncrysol.2016.05.031
0022-3093/© 2016 Elsevier B.V. All rights reserved.

Lately, Liu et al. [25] reported that the improved hydrostability was closely related to the high content of octahedrally coordinated cobalt (Co^{3+}) in the form of Co_3O_4 in silica matrices, contrary to the less hydrostable tetrahedrally coordinated cobalt (Co^{2+}). Nevertheless, the majority of the work for silica doped membranes for desalination has been limited on cobalt oxide doping and thin film coating on substrates with interlayers. Other metal dopants such as palladium [26,27], iron [28], niobia [29,30], zinc [31] and lanthanum [32] in silica membranes have been reported for gas separation membranes. Hence, there are potential opportunities to study the performance of different metal oxide silica membranes for desalination.

The impregnation of silica matrices with nickel oxide has been previously reported for microporous structures [33,34], mesoporous structures [35], hydrogen adsorption [36] and aerogel/xerogel porous structures [37]. Hence, nickel oxide silica matrices seem to be a versatile material, though not well explored for the preparation of membranes for desalination. To this end, this work investigates the evolution of higher Ni/Si molar ratios up to 50% in the structural formation of nickel oxide silica xerogels. Furthermore, the concept of interlayer-free membranes is an attractive research avenue which can significantly reduce processing time and complexity without compromising on membrane quality and stability. Therefore, this work evaluates the performance of interlayer-free nickel oxide membranes for desalination under brackish (NaCl 0.3 wt%) and seawater (NaCl 3.5 wt%) conditions.

2. Experimental section

The nickel oxide silica sol was prepared by modifying a metal oxide silica sol synthesis published elsewhere [38]. Briefly, nickel oxide sols were synthesized by the hydrolysis and condensation of tetraethyl orthosilicate (TEOS, Aldrich) in absolute ethanol (EtOH) with and without 30% aqueous H_2O_2 plus nickel nitrate hexahydrate ($Ni(NO_3)_2{\cdot}6H_2O$). An initial molar ratio of 255 EtOH: 4 TEOS: x $Ni(NO_3)_2{\cdot}6H_2O$: yH_2O_2: z H_2O was mixed and vigorously stirred for 3 h in an ice-cooled bath to avoid partial hydrolysis. The x molar concentration of $Ni(NO_3)_2{\cdot}6H_2O$ varied from 0.2, 0.4, 1, 1.4 and 2 to give Ni/Si molar ratio of 5%, 10%, 25%, 35% and 50%. The y molar of H_2O_2 was 0 and 9 only. The z molar ratio of H_2O was varied to maintain the effective water molar ratio of 40. Each sol sample was dried in a temperature-controlled oven at 60 °C under normal atmospheric conditions to form a xerogel. The xerogel samples were crushed finely and calcined at temperature 500 °C for 2 h in air with a ramp rate of 2 °C min^{-1}.

Nickel oxide silica membrane xerogels in powder form were characterised by using a Shimadzu IRAffinity-1 Fourier-transform infrared (FTIR) spectrometer with a Pike MIRacle attenuated total reflectance accessory (ATR-FTIR) at wavelength range 400–4000 cm^{-1}. All spectra were normalized using the intense peak at 1080 cm^{-1} (Si—O—Si stretching vibration). This peak was baseline resolved and observed to be the least varying peak. Deconvolution of the FTIR spectra was performed using the Fityk computer program with Gaussian peak during curve fitting. The same number of peaks was used in the entire spectral peak fitting. The half width at half maximum (HWHM) was fixed for each peak, whilst the peak position was allowed to change slightly to realize qualified fitting. The gravimetric analyses of xerogels were performed on a Shimadzu thermogravimetric analyser TGA-50 using air flow rate of 60 mL min^{-1} and heating rate 2 °C min^{-1}. Samples were degassed under vacuum for more than 6 h at 150 °C before nitrogen adsorption analysis was performed at 77 K and 1 bar using Micromeritic TriStar 3020 instrument. The specific surface area was determined from the Brunauer, Emmett and Teller (BET) method and total pore volume was taken from the last point of the isotherm. Average pore diameter (4V/A by BET) was used to determine the average pore sizes.

Thin films were directly coated on macroporous α-alumina substrates ($\phi \approx 10$ mm, Ceramic Oxide Fabricates Australia) via a dip-coating process with a dwell time of 2 min and a dipping and withdrawal rate of 10 cm min^{-1}. Each layer was calcined separately after dip coating at 500 °C in a temperature controlled furnace, with a hold time of 2 h and a ramp rate of 2 °C min^{-1}. The dip-coating and calcination procedure were repeated five times to form the top layer. The desalting performance of calcined nickel oxide silica membranes was evaluated by measuring the produced water flux and rejected salt concentration in the permeate water. The salt concentration and temperature of the feed water were kept constant. The membrane was assembled into a classical pervaporation set-up for desalination as shown in Fig. 1. The membrane was immersed in a beaker containing saline feed solution and blocked at one end with the other end connected to a cold trap (immersed in liquid nitrogen) and a vacuum pump operating at 1.5 kPa. The feed solutions were prepared with sodium chloride (NaCl) dissolved in deionised water with concentrations set at 0.3 and 3.5 wt%. The beaker was placed on a hot plate which was controlled by a thermocouple with temperature set at room temperature (~25 °C), 40 and 60 °C. The feed solution was kept under constant recirculation to prevent salt built up on the outer shell of the membrane.

The water flux, F (kg m^{-2} h^{-1}), was determined based on the equation $F = m/(A.\Delta t)$, where m is the mass of permeate (kg) retained in the cold trap, A is the active surface area (m^2) of the membrane and Δt is the time measurement (h). The salt rejection, R (%), was calculated as $R = [(C_f - C_p)/C_f] \times 100\%$, where C_f and C_p are the feed and permeate concentrations of salt (wt%). The salt concentration was determined from conductivity measurements and a generated standard curved using a conductivity meter (LabCHEM CP).

3. Results and discussion

The nitrogen adsorption isotherms of nickel doped silica xerogels are shown in Fig. 2a and b. The addition of H_2O_2 resulted in a type I isotherm as indicated by a very strong initial adsorption at very low partial pressures ($P/P° < 0.2$) followed by saturation and are thus characteristic of type I microporous materials. Interestingly, in the absence H_2O_2, nickel doped silica xerogels tended to form mesoporous materials with a higher adsorption saturation capacity above 0.4 P/P° and a hysteresis with a smooth inflection indicating a type IV isotherm. There is a general trend whereby the total pore volume increased with the Ni content, except for a typical trend for the Ni/Si 50% sample which is lower than the pore volume of Ni/Si 25% and 35% sample. Fig. 2c shows that the BET surface area for the samples with H_2O_2 varied within 10% as a function of the Ni/Si molar ratio, which is within the experimental error of 11%. Likewise, the average pore diameter shown in Fig. 2d remained constant at 2.1 ± 0.05 nm. These results strongly suggest that adding nickel oxide to the silica gel matrix with H_2O_2 maintained the microporosity of the amorphous silica xerogel. In other words, the increase in pore volumes was also accompanied by increases in the surface area. It is however interesting to observe the low BET surface area of 99 m^2 g^{-1} for the H_2O_2 Ni/Si 5% sample, resulting in a significant reduction in surface area by over 300% as compared to the other samples also prepared with H_2O_2. Similar effect has also been reported for low molar ratios of Fe/Si 2%

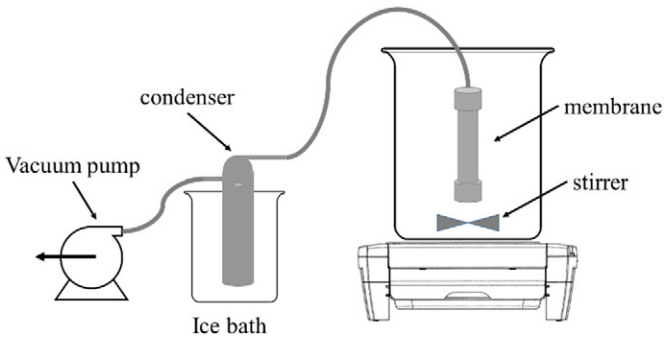

Fig. 1. Schematic of the membrane desalination pervaporation set up.

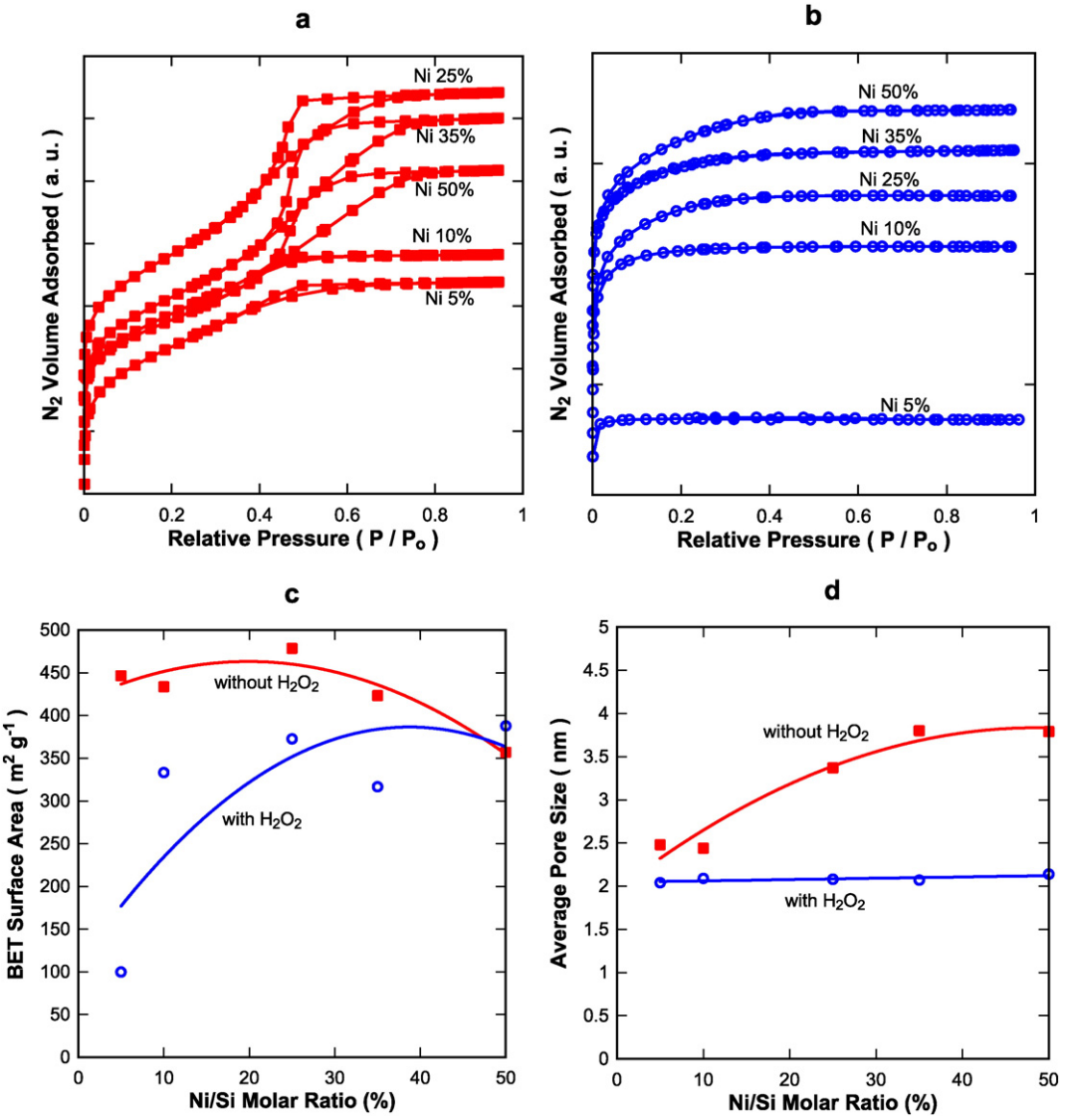

Fig. 2. Nitrogen adsorption isotherms of samples (a) without H_2O_2 and (b) with H_2O_2, (c) BET surface areas (±11%) and (d) average pore diameters (±2.5%) of nickel oxide silica xerogels (lines are provided as guides to the eyes only).

[39] and Co/Si 10% [40]. Nevertheless, the samples without H_2O_2 resulted in different trends. The mesoporosity increased significantly as a function of the Ni content as the average pore size increases whilst the BET surface area decreases for Ni/Si ratios from 25 to 50%. This effect has also been observed for cobalt oxide silica, and the increase in mesoporosity was attributed to the agglomeration of cobalt oxides [41]. Possibly, the same effect is also occurring for the increase in porosity as a function of the Ni/Si molar ratio in this work.

Fig. 3a and b display the IR spectra of xerogel samples between wavenumber 650 and 1450 cm^{-1}. The bands observed are conventionally found in silica materials which include the bands at 800 cm^{-1} and 1070 cm^{-1} with a shoulder near 1200 cm^{-1} corresponding to different modes of siloxane stretching bonds (Si—O—Si) whilst the shoulder in the region of 960 cm^{-1} is assigned to the stretching vibration of Si—OH [42–44]. Overall the peak of the Si—O band (1070 cm^{-1}) for the samples with H_2O_2 is broader than the samples without H_2O_2. To understand further the effect of the silica sol-gel reaction on the formation of functional groups of the nickel oxide silica matrices, the region between 870 and 1300 cm^{-1} were deconvoluted, allowing the calculation of a silanol (~960 cm^{-1}) to siloxane (~1070 cm^{-1}) ratio. Deconvolution results in Fig. 3c show that the silanol/siloxane ratio remained almost constant for the samples prepared without H_2O_2, and only small increments are observed as the Ni/Si ratio increases. These results suggest that nickel oxide had no effect or a marginal effect only in the sol-gel reactions without H_2O_2. However, it is interesting to note that the samples prepared with H_2O_2 exhibited a silanol/siloxane ratio twofold higher than the samples without H_2O_2. In general, the sol-gel reactions from TEOS as a silica precursor are related to hydrolysis reaction of alkoxides leading to the formation of silanol groups, and subsequently, the condensation reactions leads to the formation of siloxane bridges [45, 46]. The trend of the silanol/siloxane ratio clearly indicates that the role of H_2O_2 favoured the formation of silanol groups and slightly inhibited the condensation reactions. Contrary to this, the samples without H_2O_2 resulted in a more crosslinked nickel oxide silica structure with greater siloxane bridges and favouring the condensation reactions. Nevertheless, the H_2O_2 Ni/Si 5% sample resulted in a silanol concentration five-fold higher than those of the other samples prepared with H_2O_2. These results explain the low BET surface area of the H_2O_2 Ni/Si 5% sample observed in Fig. 2d, as higher silanol concentration favour interpenetration of silica [47,48], leading to densification and surface area reduction. This also indicates that the extent of condensation is much reduced in the H_2O_2 Ni/Si 5% sample because of the low amount of the nickel concentration, which inherently supplies the source of acid catalyst in the system.

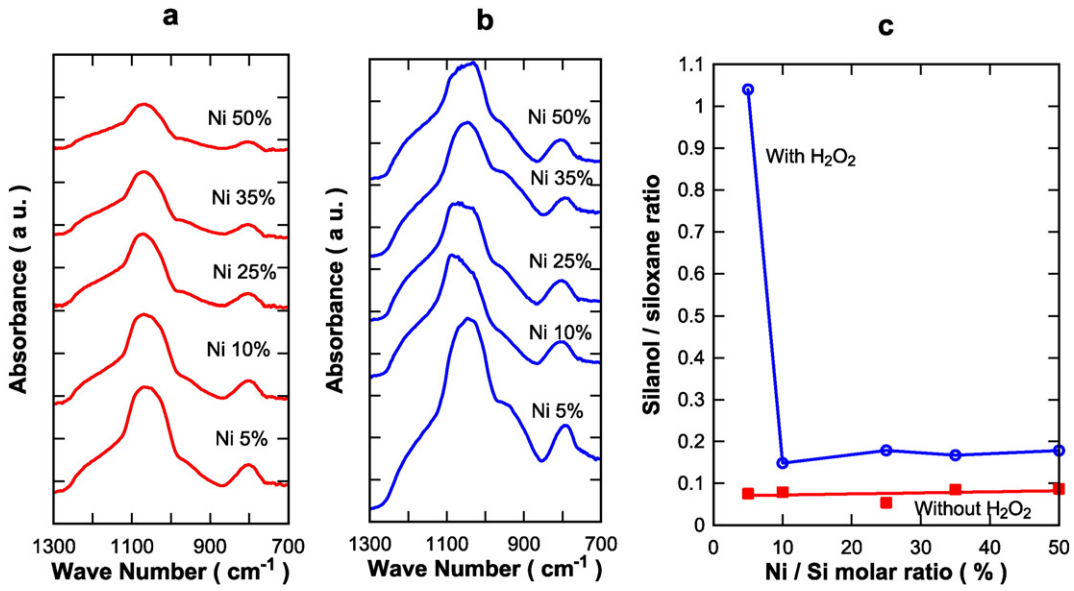

Fig. 3. FTIR spectra of samples (a) without H_2O_2 and (b) with H_2O_2; (c) silanol/siloxane ratio as of samples, as a function of Ni/Si molar ratio with H_2O_2 and without H_2O_2 with lines provided as guides to the eyes only.

Silica sol-gel reactions with H_2O_2 can generally be considered to proceed via an acid-catalysed system. As an oxidizing agent, H_2O_2 oxidizes the nickel nitrate to form HNO_3 based on the following chemical reaction (using Ni/Si = 50% as examples) [49]:

$$9H_2O_2 + 2Ni(NO_3)_2.6H_2O \rightarrow 4HNO_3 + 2NiO_2 + 12H_2O + 7H_2O_2.$$

Due to the presence of the nitric acid as a catalyst, the hydrolysis reaction involving TEOS and the water molecules is catalysed by the acid which promotes the formation of the silanol groups, and thus increases the overall concentration of the silanol concentration as evidenced by the FTIR ratio analyses. Moreover, with increasing incorporation of nickel nitrates from Ni/Si 5 to 50%, the molar concentration of nitric acid increases stoichiometrically. As a result, the initial pH value of the sol is expected to decrease with increasing nickel nitrate concentration. This is well corroborated with the measured pH shift from pH 2.62 to pH 2.05 of the 5 to 50% Ni/Si sols and in good agreement with the cobalt oxide silica sol-gel report by Elma et al. [23]. However, it should be mentioned that water (hydrolysing agent) and ethanol (solvent) molar ratios were kept constant, which should not affect the initial pH of the sol. In comparison, the initial pHs of the non-peroxidic system were recorded between pH 4 and 5, which is above the isoelectric point of the silica species (pH 1–3) [50–52], and this rendered the silica sol-gel reactions to occur in the basic environment which generally forms more siloxane bridges and mesoporous structures. Therefore, it can be remarked that H_2O_2 rendered the sol-gel process to proceed in an acidic environment catalysed by the presence of the nitric acid which favoured the formation of silanol groups and microporous materials.

The TGA mass loss curves in Fig. 4 show that H_2O_2 had a marginal effect in terms of the total mass loss, which was very similar to the samples prepared without H_2O_2. However, the content of nickel had a significant effect as the average moss loss increased from ~34% to 48% and 57% as the Ni/Si molar ratio was raised from 10% to 25% and 50%, respectively. Initial mass losses from 80 to 120 °C were consistently similar to both set of samples. This is mainly attributed to the loss of physisorbed water and ethanol molecules. Nevertheless, it is interesting to observe that H_2O_2 had a significant effect on the sample mass loss from ~150 to ~360 °C, contrary to the marginal effect of total mass loss. These effects are more noteworthy for the samples prepared with Ni/Si molar rations of 25 and 50%. For instance, the samples prepared without H_2O_2 continued to lose mass up to ~260 °C, where there is a rapid mass loss until the temperature reaches ~305 °C. From thereon, the mass loss is marginal. The samples prepared with H_2O_2 followed the same trend, though at different temperatures. For instance, mass loss continued at a constant rate up to ~260 °C, followed by a fast mass loss to ~360 °C.

The TGA results in Fig. 4 suggest that H_2O_2 has affected the sol-gel reactions during the calcination step. The decline in the mass observed from 150 to 305 or 360 °C corresponds to dehydroxylation due to the condensation of the OH groups in the silica particles [53]. The condensation reactions continued at very low rates after 305 or 360 °C, as mass losses were only minor. Likewise, the FTIR results in Fig. 4b suggest H_2O_2 has also affected the sol-gel reactions. These results clearly indicate that H_2O_2 has favoured hydrolysis reactions and inhibited to some extent the condensation reactions, thus leading to a higher relative amount of silanol groups (Si—OH). There is also a strong correlation between porosity and Si—OH groups leading to the formation of

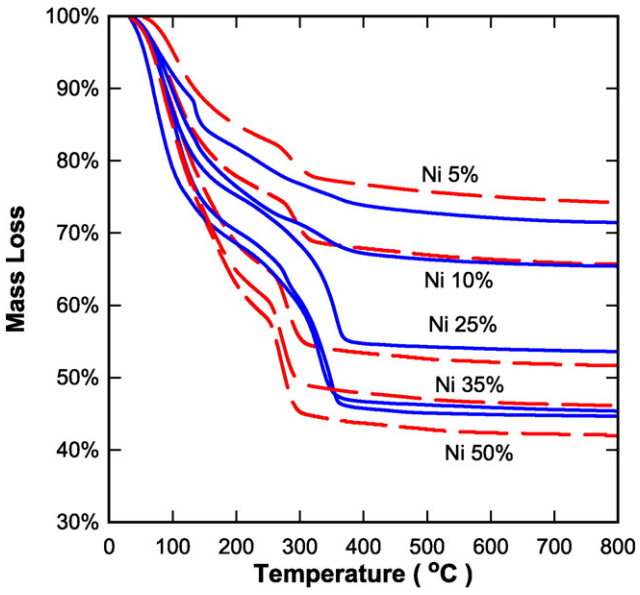

Fig. 4. Mass loss (< ± 1%) curves of samples as a function of Ni/Si molar ratio with H_2O_2 (full line ▬) and without H_2O_2 (broken line – –).

microporous structure, in line with reports elsewhere [54–57]. This can be clearly observed from the results in Fig. 2a and b, where the samples prepared with H_2O_2, which have a higher content of Si—OH group, resulted in microporous structures with smaller average pore diameters of ~2.1 nm. Contrary to this, the samples prepared without H_2O_2 had a higher content of siloxane bridges (Si—O—Si) (Fig. 3b), thus forming mesoporous structures (Fig. 2a).

Three set of Ni/Si molar concentration were chosen to prepare membranes, representing Ni/Si at low (10%), medium (25%) and high (50%) molar ratios. The performance of the membranes was initially evaluated using a brackish water (NaCl 0.3 wt%) their performance as displayed in Fig. 5. In terms of water flux, there are three trends. The first trend clearly indicates that the membranes prepared with H_2O_2 (Fig. 5a) consistently delivered lower fluxes than those prepared without H_2O_2 (Fig. 5b). These results are attributed to a dense membrane matrix, and associated with lower total pore volumes as evidenced by the nitrogen adsorption isotherms in Fig. 2. Hence, the denser nickel oxide silica matrix derived from the sol-gel synthesis containing H_2O_2 provided a higher resistance to the diffusion of water, and consequently lower water fluxes. The second trend is related to the increase of water flux as a function of temperature for all samples, though the membrane prepared with a 25% Ni/Si molar ratio and without H_2O_2 gave marginal increases in water fluxes only. In pervaporation systems such as the one used in this work, the flux of water (J) is described by $J = K\,\Delta P$ [58, 59], which is proportional to the water vapour pressure (ΔP) and a mass transfer coefficient K. Hence, by increasing the temperature, the water vapour also increases, and consequently leading to a higher driving force and water fluxes. The final trend is that the membranes prepared with 25% Ni/Si molar ratio for both sol-gel conditions (with and without H_2O_2) gave the highest water fluxes whilst 50% Ni/Si molar ratio resulted in the lowest water fluxes. These results strongly suggest that a superior structural arrangement of the amorphous silica and nickel oxide particles were reached at values ~25% Ni/Si molar ratio. This is also in line with cobalt oxide silica xerogels published elsewhere [40].

In terms of salt rejection, there are two clear trends. The first trend is that the membranes prepared with H_2O_2 generally gave slightly higher salt rejection values. This is attributed to the smaller pore sizes which correlate well with the pore size values in Fig. 2a. Nevertheless, it is interesting that the mesoporous nickel oxide silica membranes prepared without H_2O_2 were also capable of rejecting the diffusion of hydrated salts, which have much smaller hydrated ionic diameter (Cl^- 6.64 Å and Na^+ 7.16 Å) than the mesopores ($d_p > 20$ Å) silica. In principle, silica structures are amorphous and are subject to a wide pore size distribution. However, Duke and co-workers [60] used Positron Annihilation Spectroscopy and reported amorphous silica with tri-modal pore size distribution peaking at 3, 8 and 12 Å. Although different sol-gel synthesis may give varying pore size distribution, the fact is that the mesopores are not entirely linked to each other. Therefore, the smaller constriction (~3 Å) of the silica structures are able to reject hydrated salts by pore size exclusion, whilst a very small number of percolation pathways in the membrane structure allow for the diffusion of the larger hydrated salts. The second trend is related to the consistent slightly higher salt rejection for the membranes prepared with 25% Ni/Si with and without H_2O_2. Again, this is attributed to the superior structural arrangement of the amorphous silica and nickel oxide particles at this particular nickel loading.

The membranes were further tested using a seawater salt concentration (NaCl 3.5 wt%) at room temperature (25 °C). Results displayed in Fig. 6 follow the same trends as those observed in Fig. 5a and b at NaCl 0.3 wt%, though there are notable differences. First, the water fluxes consistently reduced as the salt concentration increased to 3.5 wt%. In principle, this increase causes a reduction in the driving force in the case of concentration gradients on the membrane top layer. However, in this work pressure gradient is the driving force and the variation in salt concentration does not affect significantly the vapour pressures from 0.3 to 3.5 wt% NaCl concentrations [61]. Therefore, the reduction of water fluxes is attributed to hydrated salts built up on the membrane surface, due to salt adsorption on silica materials as reported by de Lint et al. [62]. Salt rejection also slightly reduced with the increase of the feed salt concentration to 3.5 wt% NaCl. However, a notable difference is the reduction in salt concentration from 99.9% (Fig. 5) to 97% (Fig. 6) for the membranes prepared with Ni/Si molar ration of 25%. This reduction is possibly associated with structural hydroinstability of the membranes, particularly free silanols which are ever present in microporous silica [63]. These free silanols are unstrained and tend to diffuse in the silica matrix under hydrolytic conditions, causing surface and pore modification [64]. Overall, the interlayer-free nickel oxide silica membranes performed well. High fluxes up to 7 kg m^{-2} s^{-1} were measured, whilst salt rejections ranged from 91.5 to 99.9%. On a comparison basis at room temperature and sea water concentration (NaCl 3.5 wt%), the interlayer-free nickel oxide silica membrane water flux 2.5–3.8 kg m^{-2} s^{-1} are almost one order of

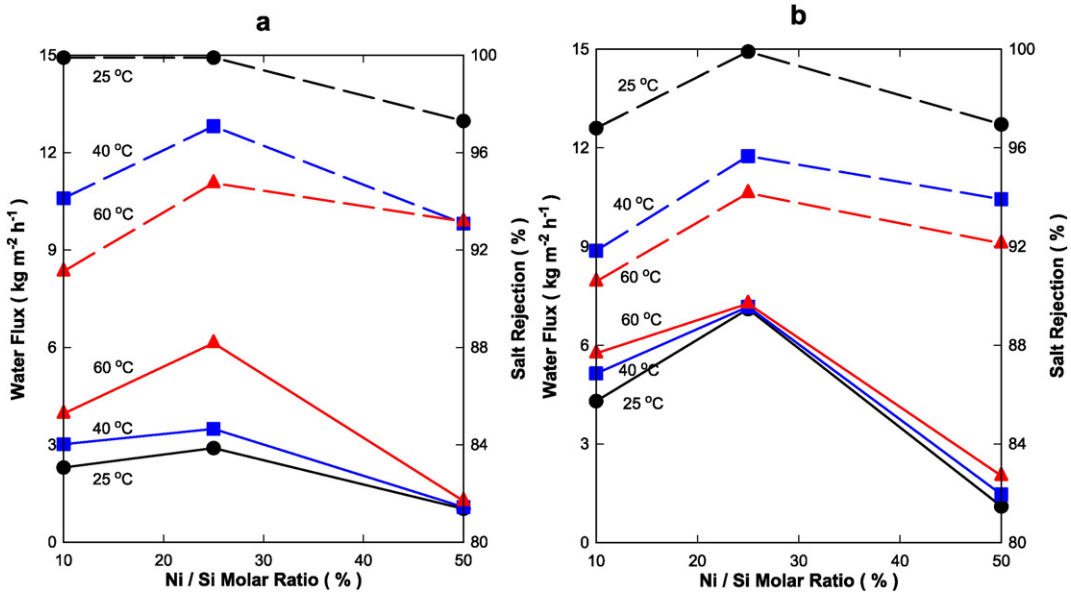

Fig. 5. Water flux (±8%) (full line ▬) and salt rejection (±1%) (broken line – –) for various temperatures at a NaCl 0.3 wt% solution as a function of the Ni/Si molar ratio for membranes prepared (a) with H_2O_2 and (b) without H_2O_2 (lines are provided guides to the eye only).

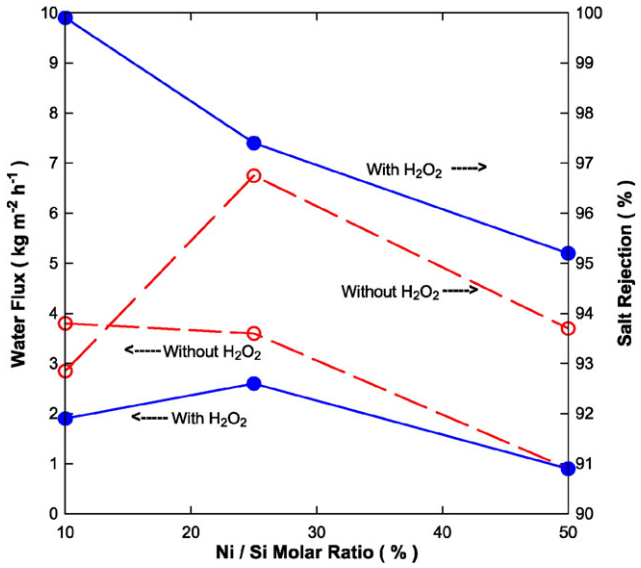

Fig. 6. Water flux (±8%) and salt rejection (±1%) for various temperatures at a NaCl 3.5 wt% solution as a function of the Ni/Si molar ratio for membranes prepared with H_2O_2 (full line ▬) and without H_2O_2 (broken line – –) (lines are provided guides to the eye only).

magnitude higher than the cobalt oxide silica membranes of 0.35, though slightly lower than recent interlayer-free cobalt oxide silica membrane of 4.2 kg m^{-2} s^{-1}.

4. Conclusions

The modified sol-gel method with and without H_2O_2 proved to meet the requirement of the preparation of interlayer-free cobalt oxide silica membranes, which in turn were able to separate water and delivering high salt rejections from 91.5 to 99.8%. Membranes prepared with Ni/Si molar ratio of 25% for both with and without H_2O_2 provided the highest water fluxes reaching values above 6 kg m^{-2} s^{-1} at 60 °C and NaCl 0.3 wt%. The membranes prepared with H_2O_2 formed denser structures with lower pore volume, which were mainly microporous, and therefore produced membranes with lower water fluxes. Contrary to this trend, membranes prepared with sol-gels without H_2O_2 were mesoporous and gave higher water fluxes. By the same token, the microporous structures gave slightly higher salt rejections than the mesoporous structures. Increasing the salt concentration from 0.3 to 3.5 wt% resulted in an overall water flux reduction, which was attributed to salt build up on the membrane surface. The salt rejection for the best membranes prepared with Ni/Si molar ratio of 25% reduced as the salt concentration increases, thus implying the onset of hydro-instability.

Acknowledgments

A. Darmawan, Y. Astuti and Sriatun gratefully acknowledge financial support from Diponegoro University via the Research for International Scientific Publications Award (Number: 315-04/UN7.5.1/PG/2015). Linda Karlina specially thanks for FIM²lab at the University of Queensland for their support for all experimental work. D. K. Wang and J. C. Diniz da Costa gratefully thank the support given by the ARC via the Discovery Early Career Researcher Award (DE150101687) and Future Fellowship Program (FT130100405), respectively.

References

[1] C.J. Vörösmarty, P. Green, J. Salisbury, R.B. Lammers, Global water resources: vulnerability from climate change and population growth, Science 289 (2000) 284–288.
[2] K.V. Reddy, N. Ghaffour, Overview of the cost of desalinated water and costing methodologies, Desalination 205 (2007) 340–353.
[3] K.P. Lee, T.C. Arnot, D. Mattia, A review of reverse osmosis membrane materials for desalination—development to date and future potential, J. Membr. Sci. 370 (2011) 1–22.
[4] J. Gilron, S. Belfer, P. Väisänen, M. Nyström, Effects of surface modification on antifouling and performance properties of reverse osmosis membranes, Desalination 140 (2001) 167–179.
[5] D. Lia, H. Wang, Recent developments in reverse osmosis desalination membranes, J. Mater. Chem. 20 (2010) 4551–4566.
[6] L. Li, J. Dong, T.M. Nenoff, R. Lee, Desalination by reverse osmosis using MFI zeolite membranes, J. Membr. Sci. 243 (2004) 401–404.
[7] L. Li, N. Liu, B. McPherson, R. Lee, Enhanced water permeation of reverse osmosis through MFI-Type zeolite membranes with high aluminum contents, Ind. Eng. Chem. Res. 46 (2007) 1584–1589.
[8] M. Drobek, C. Yacou, J. Motuzas, A. Julbe, L. Ding, J.C. Diniz da Costa, Long term pervaporation desalination of tubular MFI zeolite membranes, J. Membr. Sci. 415–416 (2012) 816–823.
[9] B. Zhu, L. Zou, C.M. Doherty, A.J. Hill, Y.S. Lin, X. Hu, H. Wang, M. Duke, Investigation of the effects of ion and water interaction on structure and chemistry of silicalite MFI type zeolite for its potential use as a seawater desalination membrane, J. Mater. Chem. 20 (2010) 4675–4683.
[10] L. Cot, A. Ayral, J. Durand, C. Guizard, N. Hovnanian, A. Julbe, A. Larbot, Inorganic membranes and solid state sciences, Solid State Sci. 2 (2000) 313–334.
[11] M.C. Duke, S. Mee, J.C. Diniz da Costa, Performance of porous inorganic membranes in non-osmotic desalination, Water Res. 41 (2007) 3998–4004.
[12] A.G. Volkov, S. Paula, D.W. Deamer, Two mechanisms of permeation of small neutral molecules and hydrated ions across phospholipid bilayers, Bioelectrochem. Bioenerg. 42 (1997) 153–160.
[13] X. Han, Y. Peng, Light-scattering characteristics of hydrated ions in dilute solutions of major sea salts, Optik 127 (2016) 1455–1459.
[14] R.K. Iler, The chemistry of silica: solubility, polymerization, Colloid and Surface Properties, and Biochemistry, Wiley, New York, 1979.
[15] A.E. Burneau, J.-P. Gallas, Vibrational spectroscopies—hydroxyl groups on silica surfaces, in: A.P.Legrand (Ed.), The Surface Properties of Silicas, John Wiley, Chichester, NY, USA, 1998.
[16] M. Elma, C. Yacou, J.C. Diniz da Costa, D. Wang, Performance and long term stability of mesoporous silica membranes for desalination, Membranes 3 (2013) 136–150.
[17] S. Wijaya, M. Duke, J.C. Diniz da Costa, Carbonised template silica membranes for desalination, Desalination 236 (2009) 291–298.
[18] Y.T. Chua, C.X.C. Lin, F. Kleitz, S. Smart, Synthesis of mesoporous carbon–silica nanocomposite water-treatment membranes using a triconstituent co-assembly method, J. Mater. Chem. A 3 (2015) 10480–10491.
[19] M. Elma, D. Wang, C. Yacou, J.C. Diniz da Costa, Interlayer-free P123 carbonised template silica membranes for desalination with reduced salt concentration polarisation, J. Membr. Sci. 475 (2015) 376–383.
[20] R. Xu, J. Wang, M. Kanezashi, T. Yoshioka, T. Tsuru, Development of robust organosilica membranes for reverse osmosis, Langmuir 27 (2011) 13996–13999.
[21] Y.T. Chua, C.X.C. Lin, F. Kleitz, X.S. Zhao, S. Smart, Nanoporous organosilica membrane for water desalination, Chem. Comm. 49 (2013) 4534–4536.
[22] C.X.C. Lin, L. Ding, K. Simon, S. S., J.C.D. da Costa, Cobalt oxide silica membranes for desalination, J. Coll. Interface Sci. 368 (2012) 70–76.
[23] M. Elma, D.K. Wang, C. Yacou, J. Motuzas, J.C.D. da Costa, High performance interlayer-free mesoporous cobalt oxide silica membranes for desalination applications, Desalination 365 (2015) 308–315.
[24] R. Igi, T. Yoshioka, Y.H. Ikuhara, Y. Iwamoto, T. Tsuru, Characterisation of co-doped silica for improved hydrothermal stability and application to hydrogen separation membranes at high temperatures, J. Am. Ceram. Soc. 91 (2008) 2975–2981.
[25] L. Liu, D.K. Wang, D.L. Martens, S. Smart, J.C. Diniz da Costa, Influence of the cobalt phase sol-gel conditioning on the hydrothermal stability of cobalt doped silica membranes, J. Membr. Sci. 475 (2015) 425–432.
[26] M. Kanezashi, C. Shimada, M. Sano, T. Yoshioka, T. Tsuru, Hydrogen permeation performance and hydrothermal stability for sol-gel derived Pd-doped silica membranes, Kagaku Kogaku Ronbun 36 (2010) 472–479.
[27] B. Ballinger, J. Motuzas, S. Smart, J.C. Diniz da Costa, Palladium cobalt binary doping of molecular sieving silica membranes, J. Membr. Sci. 451 (2014) 185–191.
[28] A. Darmawan, J. Motuzas, S. Smart, A. Julbe, J.C.D. da Costa, Temperature dependent transition point of purity versus flux for gas separation in Fe/Co-Silica membranes, Sep. Purif. Technol. 151 (2015) 284–291.
[29] V. Boffa, J.E. ten Elshof, D.H.A. Blank, Hydrothermal stability of microporous silica and niobia-silica membranes, J. Membr. Sci. 319 (2008) 256–263.
[30] V. Boffa, J.E. ten Elshof, A.V. Petukhov, D.H. Blank, Microporous niobia-silica membrane with very low CO_2 permeability, ChemSusChem 1 (2008) 437–443.
[31] L. Naszalyi, F. Bosc, A. El Mansouri, A. van der Lee, D. Cot, Z. Hórvölgyi, A. Ayral, Sol-gel-derived mesoporous SiO_2/ZnO active coating and development of multifunctional ceramic membranes, Sep. Pur. Technol. 59 (2008) 304–330.
[32] B. Ballinger, J. Motuzas, S. Smart, J.C. Diniz da Costa, Redox effect on binary lanthanum cobalt silica membranes with enhanced silicate formation, J. Membr. Sci. 489 (2015) 220–226.
[33] M. Kanezashi, M. Asaeda, Hydrogen permeation characteristics and stability of Ni-doped silica membranes in steam at high temperature, J. Membr. Sci. 271 (2006) 86.
[34] M. Kanezashi, T. Fujita, M. Asaeda, Nickel-doped silica membranes for separation of heluim from organic gas mixtures, Sep. Sci. Technol. 40 (2005) 225.
[35] X. Liu, C.-M. Chun, I.A. Aksay, W.-H. Shih, Synthesis of mesostructured nickel oxide with silica, Ind. Eng. Chem. Res. 39 (2000) 684–692.

[36] Y. Ikuhara, H. Mori, T. Saito, Y. Iwamoto, High-temperature hydrogen adsorption properties of precursor-derived nickel nanoparticle-dispersed amorphous silica, J. Am. Ceram. Soc. 90 (2007) 546.
[37] M.F. Casula, A. Corrias, G. Paschina, Nickel oxide–silica and nickel–silica aerogel and xerogel nanocomposite materials, J. Mater. Res. 15 (2000) 2187–2194.
[38] D. Uhlmann, S. Smart, J.C. Diniz da Costa, High temperature steam investigation of cobalt oxide silica membranes for gas separation, Sep. Purif. Technol. 76 (2010) 171–178.
[39] A. Darmawan, S. Smart, A. Julbe, J.C. Diniz da Costa, Iron oxide silica derived from sol-gel synthesis, Materials 4 (2011) 448–456.
[40] C. Yacou, S. Smart, J.C. Diniz da Costa, Long term performance of a multi-tube cobalt oxide silica membrane at high temperatures for gas separation, Energy Env. Sci. 5 (2012) 5820–5832.
[41] D.C.L. Vasconcelos, E.H.M. Nunes, M. Houmard, J. Motuzas, J.F. Nascimento, W. Grava, V.S.T. Ciminelli, J.C. Diniz Da Costa, W.L. Vasconcelos, Structural investigation of cobalt-doped silica derived from sol-gel synthesis, J. Non-Cryst. Solids 378 (2013) 1–6.
[42] A. Duran, C. Serna, V. Fornes, J.M. Fernadez Navarro, Structural considerations about SiO_2 glasses prepared by sol-gel, J. Non-Cryst. Solids 82 (1986) 69–77.
[43] A. Bertolluzza, C. Gagnano, M.A. Morelli, V. Gottardi, M. Guglielmi, Raman and Infrared spectra of silica gel evolving toward glass, J. Non-Crist. Solids 48 (1982) 117–128.
[44] R.F.S. Lenza, E.H.M. Nunes, D.C.L. Vasconcelos, W.L. Vasconcelos, Preparation of sol–gel silica samples modified with drying control chemical additives, J. Non-Cryst. Solids 423 (2015) 35–40.
[45] A.J. Vega, G.W. Scherer, Study of structural evolution of silica gel using ^{1}H and ^{29}Si NMR, J. Non-Cryst. Solids 111 (1989) 153–166.
[46] C.J. Brinker, A.J. Hurd, P.R. Schunk, G.C. Frye, C.S. Ashley, Review of sol-gel thin film formation, J. Non-Cryst. Solids 147&148 (1992) 424–436.
[47] C.J. Brinker, G.W. Scherer, Sol Gel Science: The Physics and Chemistry of the Sol Gel Processing, 1990Academic Press, San Diego, USA, 1990.
[48] T.A. Witten, M.E. Gates, Tenuous structures from disorderly growth process, Science 232 (1986) 1607–1612.
[49] S. Patai, The Chemistry of Peroxides, Wiley, Chichester, New York, USA, 1983.
[50] W.J. Elferink, B.N. Nair, R.M. de Vos, K. Keizer, H. Verweij, Sol-gel synthesis and characterization of microporous silica membranes: II. Tailor-making porosity, J. Coll. Interface Sci. 180 (1996) 127–134.
[51] B.N. Nair, J.W. Elferink, K. Keizer, H. Verweij, Preparation and structure of microporous silica membranes, J. Sol-Gel Sci. Technol. 8 (1997) 471–475.
[52] R. Leboda, E. Mendyk, V.A. Tertykh, Effect of medium pH on hydrothermal treatment of silica gels (xerogels) in an autoclave, Mater. Chem. Phys. 43 (1996) 53–58.
[53] P.D. Maniar, A. Navrotsky, E.M. Rabinovich, J.Y. Ying, J.B. Benziger, Energetics and structure of sol-gel silicas, J. Non-Cryst. Solids 124 (1990) 101–111.
[54] R.S.A. de Lange, J.H.A. Hekkink, K. Keizer, A.J. Burggraaf, Formation and characterisation of supported microporous ceramic membranes prepared by sol-gel modification techniques, J. Mem. Sci. 99 (1995) 57–75.
[55] B.N. Nair, T. Yamaguchi, T. Okubo, H. Suematsu, K. Kaizer, S.I. Nakao, Sol-gel synthesis of molecular sieving silica membranes, J. Membr. Sci. 135 (1997) 237–243.
[56] R.M. de Vos, H. Verweij, Improved performance of silica membranes for gas separation, J. Membr. Sci. 143 (1998) 37–51.
[57] C. Tsai, S. Tam, Y. Lu, C.J. Brinker, Dual-layer asymetric microporous silica membranes, J. Membr. Sci. 169 (2000) 255–268.
[58] K.W. Lawson, D.R. Lloyd, Membrane distillation, J. Membr. Sci. 124 (1997) 1–25.
[59] A.M. Alklaibi, The potential of membrane distillation as a stand-alone desalination process, Desalination 223 (2008) 375–385.
[60] M.C. Duke, S.J. Pas, A.J. Hill, Y.S. Lin, J.C. Diniz da Costa, Exposing the molecular sieving architecture of amorphous silica using positron annihilation spectroscopy, Adv. Funct. Mater. 18 (2008) 3818–3826.
[61] Y.T. Chua, G. Ji, G. Birkett, C.X.C. Lin, F. Kleitz, S. Smart, Nanoporous organosilica membrane for water desalination: theoretical study on the water transport, J. Membr. Sci. 482 (2015) 56–66.
[62] W.B.S. de Lint, T. Zivkovic, N.E. Benes, H.J.M. Bouwmeester, D.H.A. Blank, Electrolyte retention of supported bi-layered nanofiltration membranes, J. Membr. Sci. 277 (2006) 18–27.
[63] C. Cannas, M. Casu, A. Musinu, G. Piccaluga, ^{29}Si CPMAS NMR and near-IR study of sol–gel microporous silica with tunable surface area, J. Non-Cryst. Solids 351 (2005) 3476–3482.
[64] M.C. Duke, J.C.D. da Costa, D.D. Do, P.G. Gray, G.Q. Lu, Hydrothermally robust molecular sieve silica for wet gas separation, Adv. Funct. Mater. 16 (2006) 1215–1220.